Electronic Supplementary Material (ESI) for RSC Advances.

Supporting Information

Nanoporous polymer scaffold-embedded nonwoven composite separator membranes for high-rate lithium-ion batteries

Jung-Hwan Kim,[a] Jeong-Hoon Kim,[a] Eun-Sun Choi,[b] Jong Hun Kim,[b] and Sang-Young Lee*[a]

[a]*Department of Energy Engineering, School of Energy and Chemical Engineering Ulsan National Institute of Science and Technology (UNIST), Ulsan, 689-798, Korea*

[b]*Batteries R&D, LG Chem, Yusong-gu, Daejon, 305-380, Korea*

Figure S1. An overview of stepwise fabrication procedure of SF-NW separators, wherein a FE-SEM photograph of a pristine PET nonwoven is provided.

Figure S2. A schematic illustration describing SiO_2/PVdF-HFP composition ratio-dependent structural variation of SF-NW separators and its influence on ionic transport.

Figure S3. (a) Photographs showing liquid electrolyte (1 M $LiPF_6$ in EC/DEC = 1/1 v/v) wetting behavior; (b) Thermal shrinkage of various SF-NW separators and PP/PE/PP separator after exposure to 150 ^oC for 0.5 h.

Figure S4. Linear sweep voltammograms of SF-NW separator (SiO_2/PVdF-HFP = 90/10 w/w) and PP/PE/PP separator at a voltage scan rate of 1.0 mV s^{-1}.

Fig. S5. Cyclic voltammograms of SF-NW separator (SiO_2/PVdF-HFP = 90/10 w/w) and PP/PE/PP separator at a voltage scan rate of 0.1 mV s^{-1}.

Fig. S6. Surface morphology of separators (after going through the test of charge rate capability): (a) PP/PE/PP separator; (b) SF-NW separator.

Figure S7. A FE-SEM photograph verifying long-term, structural stability of SF-NW separator (SiO_2/PVdF-HFP = 90/10 w/w) after 100^{th} cycle.

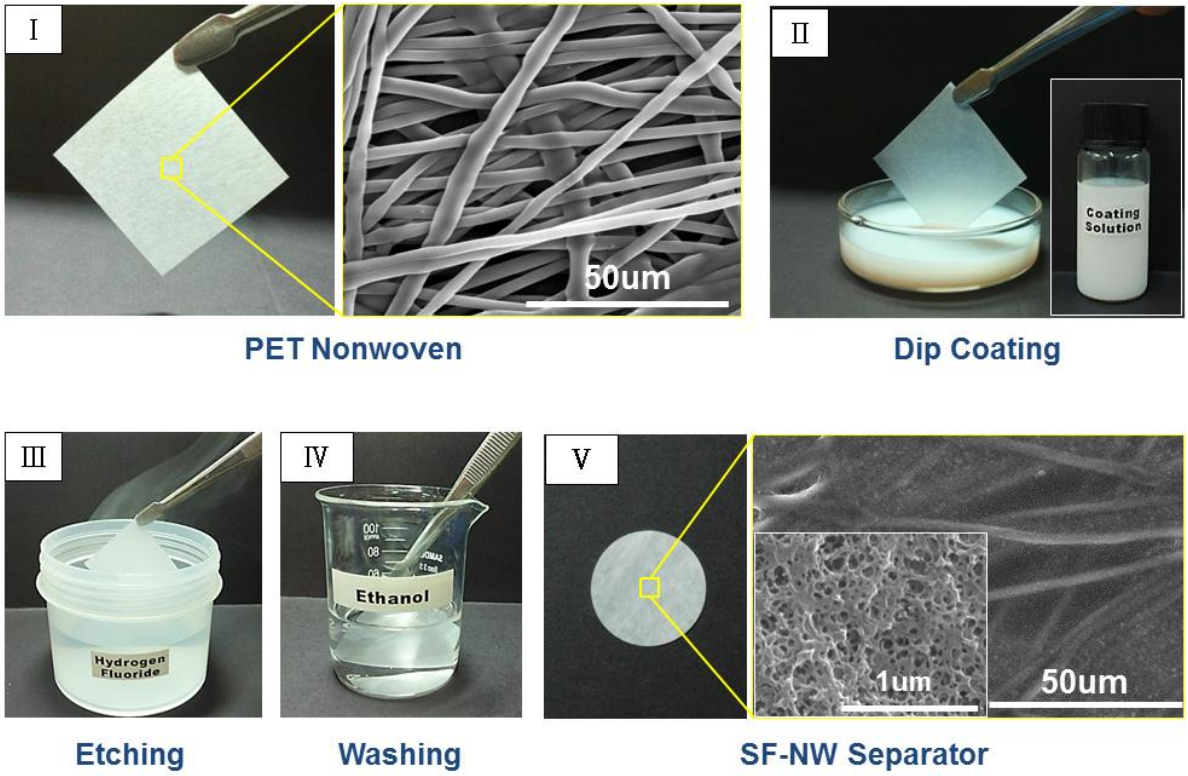

Fig. S1. An overview of stepwise fabrication procedure of SF-NW separators, wherein a FE-SEM photograph of a pristine PET nonwoven is provided.

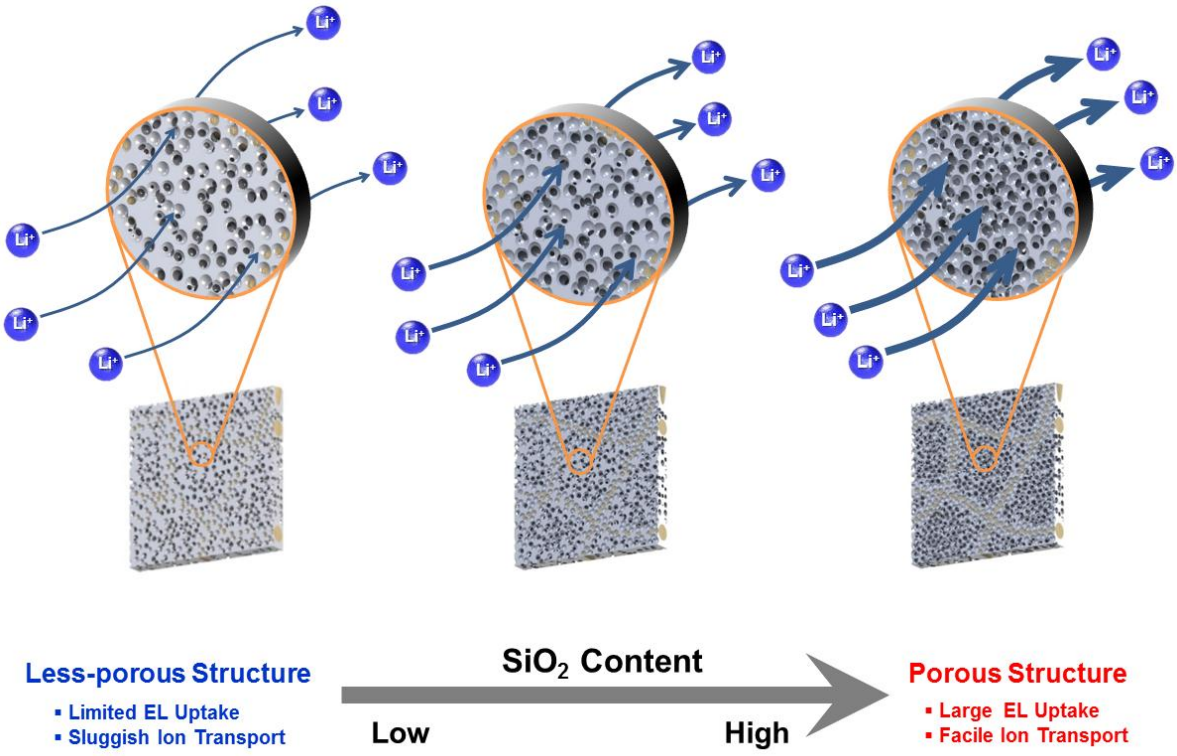

Fig. S2. A schematic illustration describing SiO_2/PVdF-HFP composition ratio-dependent structural variation of SF-NW separators and its influence on ionic transport.

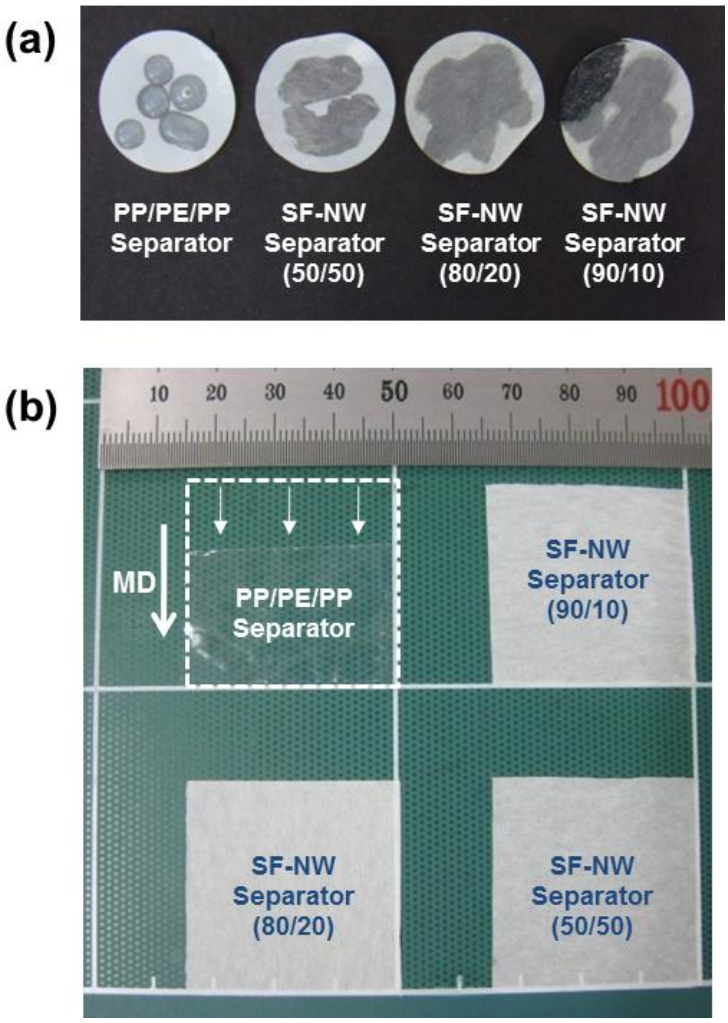

Fig. S3. (a) Photographs showing liquid electrolyte (1 M $LiPF_6$ in EC/DEC = 1/1 v/v) wetting behavior; (b) Thermal shrinkage of various SF-NW separators and PP/PE/PP separator after exposure to 150 ^{o}C for 0.5 h.

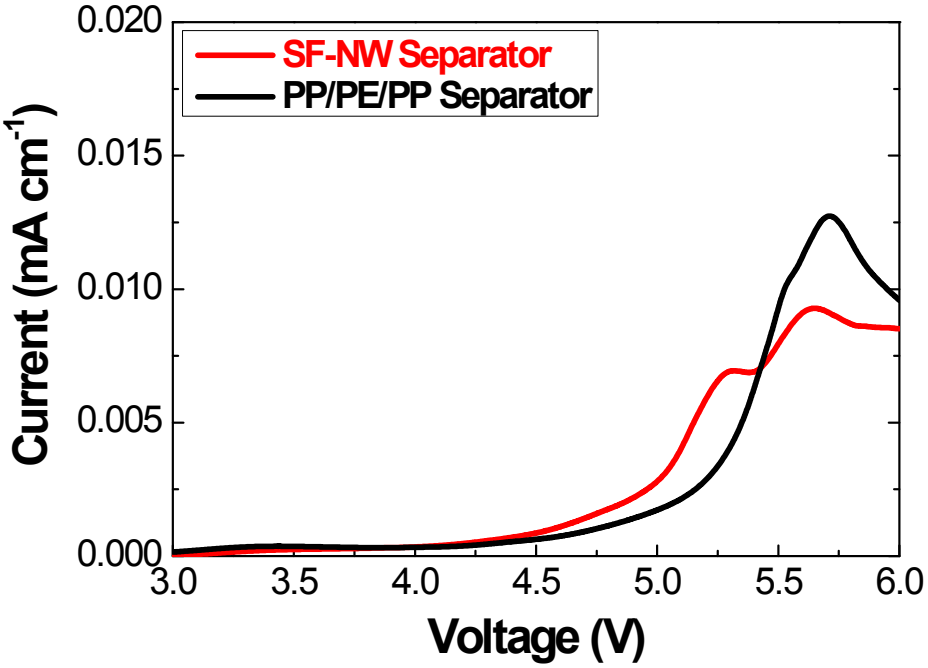

Fig. S4. Linear sweep voltammograms of SF-NW separator (SiO_2/PVdF-HFP = 90/10 w/w) and PP/PE/PP separator at a voltage scan rate of 1.0 mV s^{-1}.

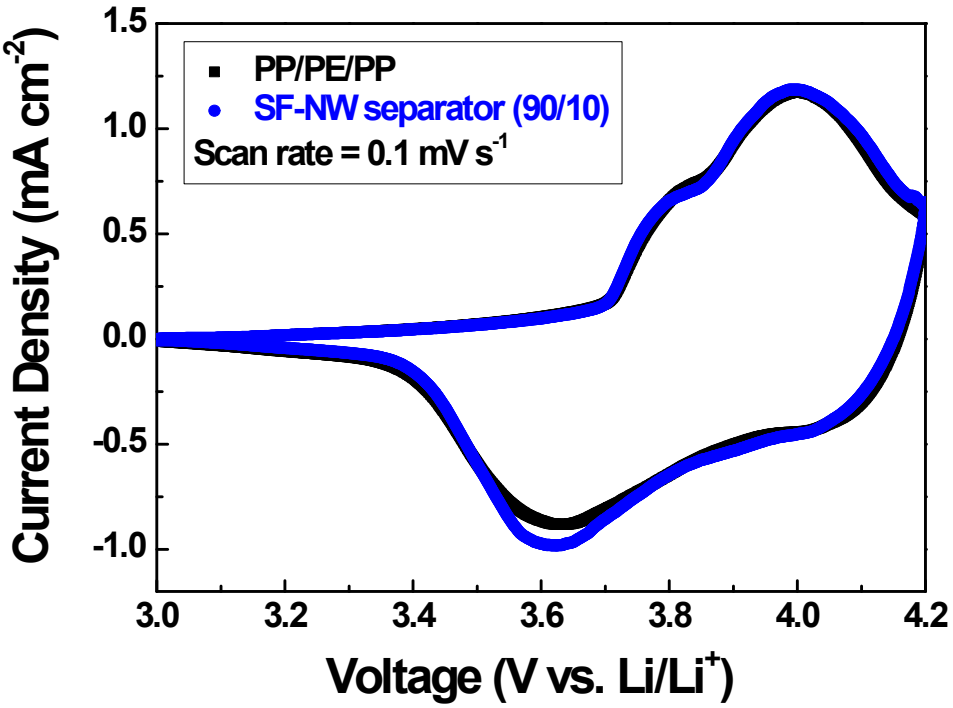

Fig. S5. Cyclic voltammograms of SF-NW separator (SiO_2/PVdF-HFP = 90/10 w/w) and PP/PE/PP separator at a voltage scan rate of 0.1 mV s^{-1}.

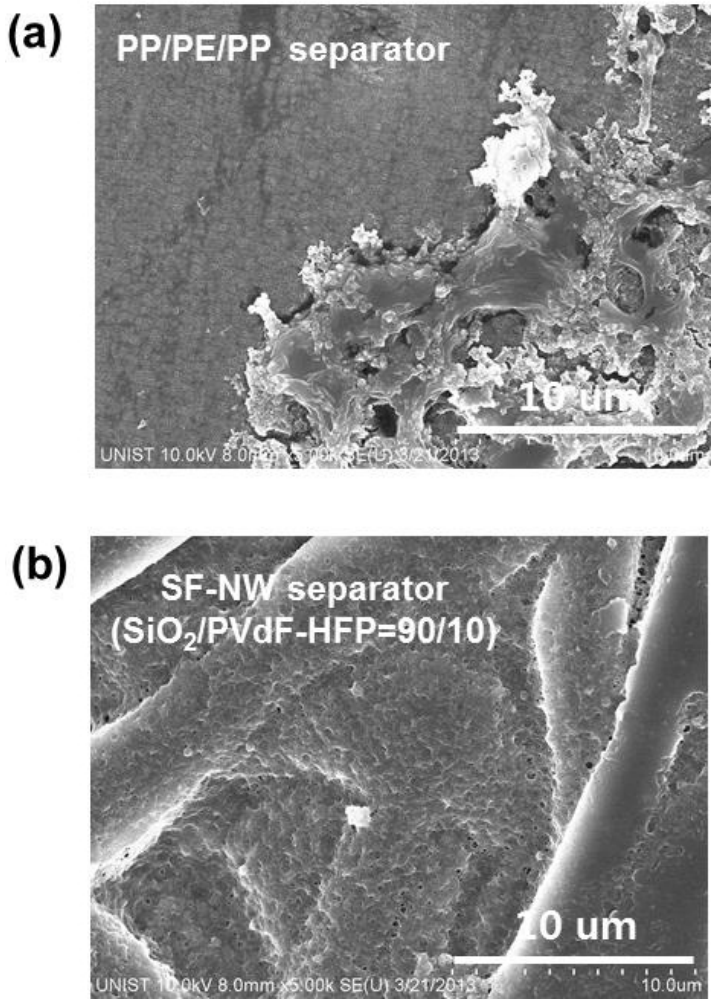

Fig. S6. Surface morphology of separators (after going through the test of charge rate capability): (a) PP/PE/PP separator; (b) SF-NW separator.

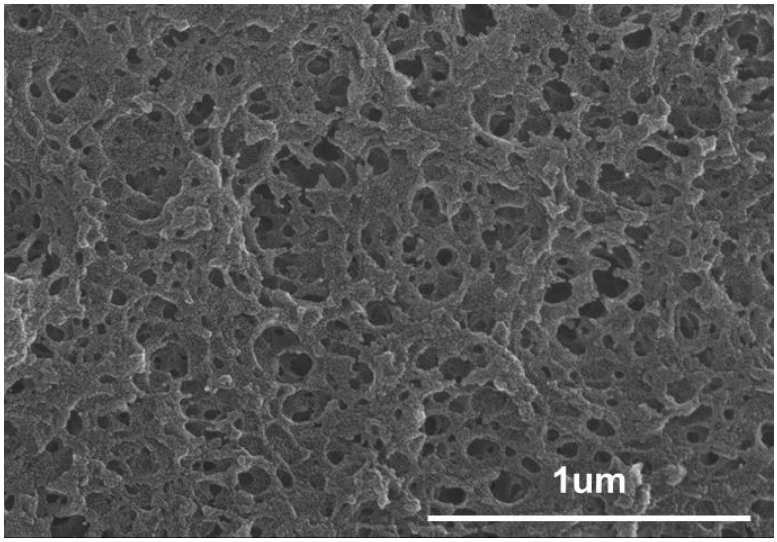

Fig. S7. A FE-SEM photograph verifying long-term, structural stability of SF-NW separator (SiO_2/PVdF-HFP = 90/10 w/w) after 100^{th} cycle.